pubs.acs.org/acschemicalbiology

Articles

Development of a Broadly Applicable Cas12a-Linked Beam Unlocking Reaction for Sensitive and Specific Detection of Respiratory Pathogens Including SARS-CoV-2

Yu Wang,[¶] Donglan Liu,[¶] Huihuang Lin,[¶] Dingbin Chen, Jing Sun, Yusang Xie, Xinjie Wang, Peixiang Ma, Yan Nie, Hong Mei, Baihui Zhao, Xingxu Huang, Ge Jiang, Xianxing Jiang,* Jieming Qu,* Jincun Zhao,* and Jia Liu*

Cite This: https://dx.doi.org/10.1021/acschembio.0c00840

Read Online

ACCESS | Metrics & More | Article Recommendations | Supporting Information

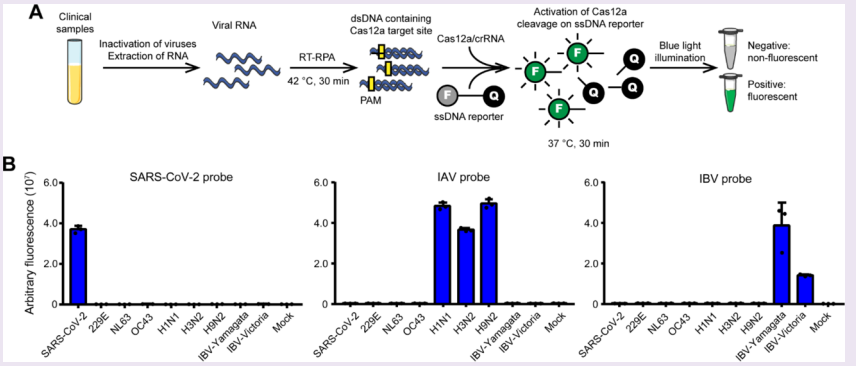

ABSTRACT: The outbreak of novel coronavirus SARS-CoV-2 has caused a worldwide threat to public health. COVID-19 patients with SARS-CoV-2 infection can develop clinical symptoms that are often confused with the infections of other respiratory pathogens. Sensitive and specific detection of SARS-CoV-2 with the ability to discriminate from other viruses is urgently needed for COVID-19 diagnosis. Herein, we streamlined a highly efficient CRISPR-Cas12a-based nucleic acid detection platform, termed **Cas**12a-**li**nked **b**eam **u**nlocking **r**eaction (CALIBURN). We show that CALIBURN could detect SARS-CoV-2 and other coronaviruses and influenza viruses with little cross-reactivity. Importantly, CALIBURN allowed accurate diagnosis of clinical samples with extremely low viral loads, which is a major obstacle for the clinical applications of existing CRISPR diagnostic platforms. When tested on the specimens from SARS-CoV-2-positive and negative donors, CALIBURN exhibited 73.0% positive and 19.0% presumptive positive rates and 100% specificity. Moreover, unlike existing CRISPR detection methods that were mainly restricted to respiratory specimens, CALIBURN displayed consistent performance across both respiratory and nonrespiratory specimens, suggesting its broad specimen compatibility. Finally, using a mouse model of SARS-CoV-2 infection, we demonstrated that CALIBURN allowed detection of coexisting pathogens without cross-reactivity from a single tissue specimen. Our results suggest that CALIBURN can serve as a versatile platform for the diagnosis of COVID-19 and other respiratory infectious diseases.

Coronavirus disease 2019 (COVID-19)[1,2] has become a public health emergency of international concern[3] since late 2019. As of January 5, 2021, the World Health Organization (WHO) has reported more than 84 million cases of COVID-19 worldwide.[3] Importantly, COVID-19 patients may have no evident clinical symptoms even when diagnosed with advanced technologies such as chest computed tomography (CT) or radiography.[4,5] Furthermore, with cough and fever being the most commonly recognized symptoms,[6] COVID-19 can be confused with the infections of other respiratory pathogens such as influenza viruses.[7] Patients with coinfecting SARS-CoV-2 and influenza viruses have also been reported.[8] The clinical complications of COVID-19 underscore the importance of molecular diagnosis.

The pathogen that causes COVID-19 is a betacoronavirus, known as severe acute respiratory syndrome coronavirus 2 (SARS-CoV-2).[9] Like other coronaviruses,[10] SARS-CoV-2 is single-stranded, positive-sense RNA virus. SARS-CoV-2 shares 79% and 50% nucleotide identity with SARS-CoV and Middle East respiratory syndrome coronavirus (MERS-CoV), respec-

Received: October 28, 2020
Accepted: February 2, 2021

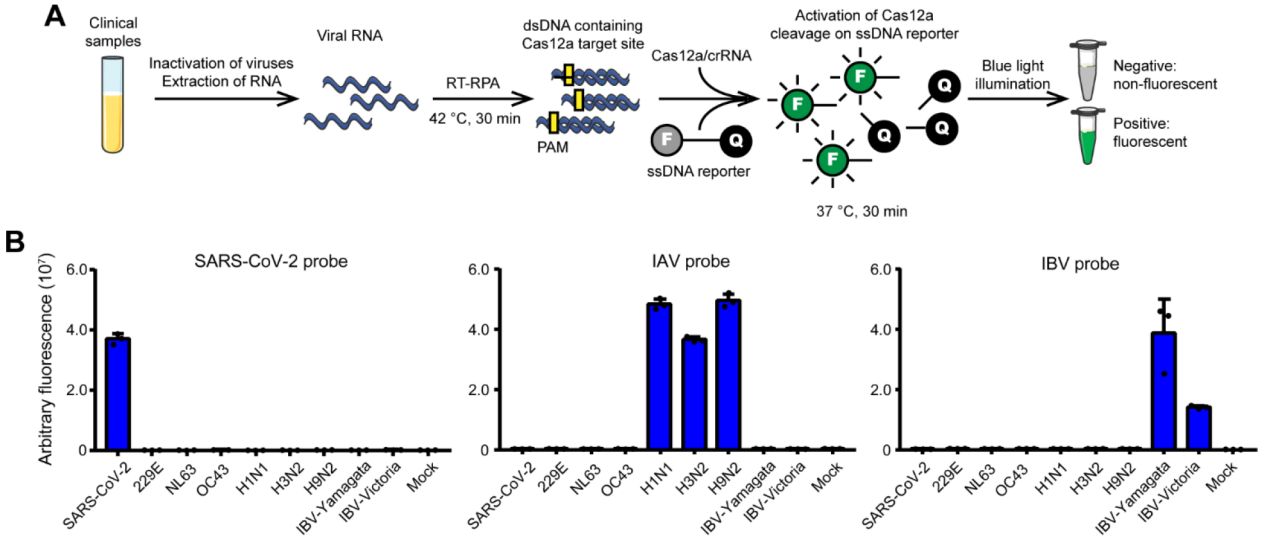

Figure 1. Specific detection of SARS-CoV-2, IAV, and IBV. (A) Schematic illustration of CALIBURN and coupled RT-RPA reaction. F, fluorophore. Q, quencher. (B) Investigation of the specificity of CALIBURN on each pathogen. For each virus, 5 μL of the extracted nucleic acids is added to each reaction without dilution. The viral copies are in the range of 10^6−10^7 per reaction for different viruses. The RT-RPA primers are SARSCoV2-S-FWD-1/SARSCoV2-S-REV-1 for SARS-CoV-2, IAV-M-FWD/IAV-M-REV for IAV, and IBV-HA-FWD/IBV-HA-REV for IBV, respectively (Table S1). The crRNA probes are SARSCoV2-S-crRNA2 for SARS-CoV-2, IAV-M-crRNA3 for IAV, and IBV-HA-crRNA4 for IBV, respectively (Table S2). The data from three biological replicates are shown as mean ± SD.

tively.[11,12] At present, reverse transcription PCR (RT-PCR)-based technologies are the most widely used molecular diagnosis methods for SARS-CoV-2.[13,14] Genes E, N, and ORF1ab of SARS-CoV-2 are commonly used targets for the design of RT-PCR probes.[15,16] High-throughput RT-PCR platforms can be developed to facilitate large-scale[17] or pooled[18] diagnosis.

Recent studies have highlighted clustered regularly interspaced short palindromic repeats (CRISPR) as affordable and field-deployable methods for the molecular diagnosis of viral nucleic acids.[19,20] CRISPR and CRISPR-associated genes (Cas) are the bacterial immune system for defending viral infections.[21−23] The modular features make CRISPR a widely used technology for genome engineering.[24−28] CRISPR-based nucleic acid detection such as SHERLOCK or DETECTR relies on the RNA-[20,29] or DNA-targeting[30] activities of Cas nucleases. Different CRISPR-Cas systems can be combined to enable multiplexed viral detection.[31] Specifically, CRISPR-Cas12a-based methods have been harnessed for the rapid detection of both nucleic acid[30,32−34] and non-nucleic acid[35,36] molecules. Cas12a-based detection technologies can facilitate the diagnosis of emerging pathogens including African Swine Fever virus (ASFV).[37−40]

During the outbreak of COVID-19, Cas12a-based SARS-CoV-2 detection platforms have been developed.[41−43] However, the efficiencies of CRISPR detection across different respiratory pathogens have not been well characterized. In addition, the effects of specimen types on detection are poorly understood. In the present study, we developed a CRISPR-Cas12a-based nucleic acid detection platform, which we termed Cas12a-linked beam unlocking reaction (CALIBURN), for the sensitive and specific detection of respiratory pathogens including SARS-CoV-2. We evaluated the performance of CALIBURN on SARS-CoV-2 and other coronaviruses and influenza viruses with the consideration of specimen types. Moreover, we investigated the ability of CALIBURN for the parallel detection of multiple pathogens from tissue samples of the SARS-CoV-2 mouse model.

RESULTS AND DISCUSSION

General Procedure of CALIBURN. The general procedure of CALIBURN is shown in Figure 1a. Briefly, clinical samples are inactivated and then extracted for viral RNA. The RNA is reverse transcribed (RT) and then amplified by recombinase polymerase amplification (RPA) into double-stranded DNA (dsDNA).[44] The RT-RPA products are subjected to Cas12a cleavage reaction where CRISPR RNA (crRNA) guides the nuclease to bind to the amplified dsDNA, unleashing its indiscriminate single-stranded DNA (ssDNA) cleavage activity. Cleavage of the ssDNA reporter by the collateral activity of Cas12a unlocks the fluorescence of uncoupled fluorophore. CALIBURN is different from previous CRISPR-based nucleic acid detection platforms with three major improvements: first, RT-RPA primers are optimized by determining their efficiencies in generating RT-RPA product that yields optimal fluorescence signal during Cas12a cleavage of ssDNA reporter; second, selected RT-RPA primers and crRNA probes are examined for their mutual specificity on the target pathogen and other pathogens to ensure the orthogonality of the reaction; third, the readout of CALIBURN is determined as fluorescence intensity and reported positive or negative according to threshold signal.

Normalizing the Efficiency of CALIBURN by the Active Units of Purified Cas12a Proteins. We first investigated the effects of Cas12a protein quality on the efficiency of CALIBURN. We purified three batches of Cas12a proteins with different procedures. These proteins had homogeneity of more than 90% and different values of OD_{260} over OD_{280} (Figure S1A). Using a dsDNA substrate as the mimic for reverse transcribed ORF1ab gene of SARS-CoV-2, we found that CALIBURN with equal molar concentrations of different Cas12a preparations yielded notably different fluorescence signal (Figure S1B). To normalize the Cas12a

https://dx.doi.org/10.1021/acschembio.0c00840
ACS Chem. Biol. XXXX, XXX, XXX−XXX

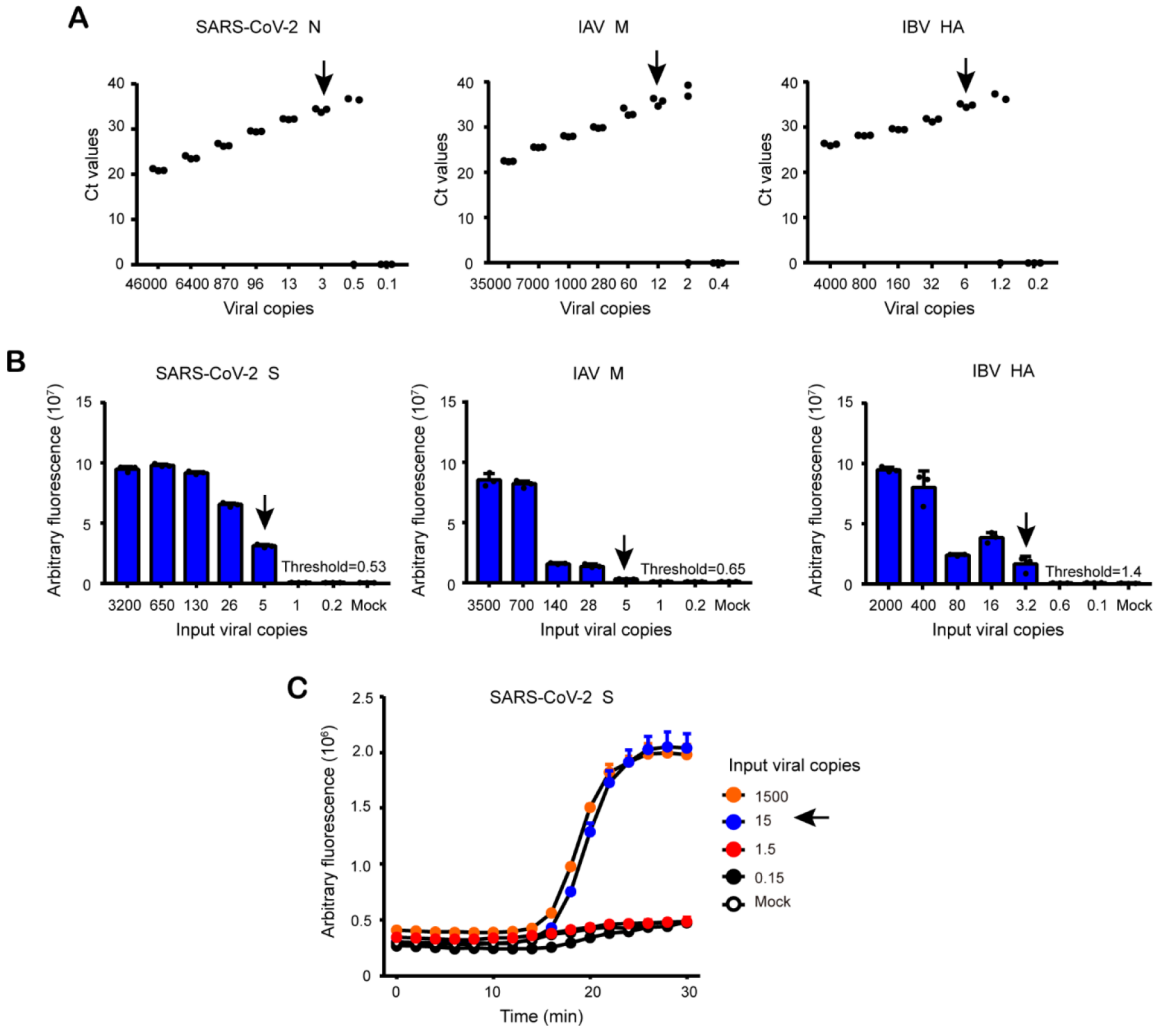

Figure 2. LODs of different methods on detecting laboratory strains of SARS-CoV-2, IAV, and IBV. (A) RT-PCR. Positive signal is determined by valid C_t values. (B) CALIBURN. Viral RNA of indicated copies is added to 5 μL RT-RPA reactions and the reaction product is directly transferred to Cas12a reaction with a final volume of 20 μL. The threshold of positive signal is set as the mean plus 3-fold standard deviation (mean+3σ) of the mock sample. (C) Fluorescent RT-RPA alone without CALIBURN reaction for detection of SARS-CoV-2. Arrows denote LOD, as defined by the lowest input viral copies resulting in positive signal readouts with more than 95% confidence. The data are shown as mean ± SD (n = 3). The RT-RPA primers and crRNA probes are identical to those in Figure 1.

activity in CALIBURN, we used an *in vitro* cleavage (IVC) assay to determine the active units of purified Cas12a proteins (Figure S1C). One activity unit of Cas12a was defined as the amount of proteins required to completely cleave 1 pmol dsDNA within 1 h in a 20 μL reaction at 37 °C. Detection of ORF1ab dsDNA by CALIBURN with 0.07 units of Cas12a from different preparations resulted in similar fluorescence without significant difference (Figure S1D), thereby justifying the use of Cas12a active unit for subsequent experiments.

Analyses of Experimental Factors Affecting the Efficiency of CALIBURN. To optimize CALIBURN, we examined the effects of dsDNA substrate, reaction time, and Cas12a concentration on the fluorescence signal. These experiments were carried out using ORF1ab dsDNA substrate and all three preparations of Cas12a proteins. Under fixed incubation time of 120 min and Cas12a concentration of 0.05 units, the fluorescence of CALIBURN displayed an S-shape curve against dsDNA concentration, with the plateau achieved at approximately 1 nM (Figure S2A). When Cas12a and dsDNA are fixed to 0.05 units and 1 nM, respectively, the fluorescence of CALIBURN exhibited time-dependent progression within the monitored time course of 120 min (Figure S2B). Under 1 nM dsDNA and 120 min incubation time, the CALIBURN fluorescence displayed a bell-shaped curve when Cas12a protein ranged from 0.01 units to 0.3 units, with a peak signal at 0.07 units (Figure S2C). Interestingly, a previous study also reported the inhibition of activated fluorescence at high Cas12a concentration.[37] To confirm that the inhibited CALIBURN fluorescence was due to excess ratio of Cas12a over dsDNA substrate, we performed another assay where the ratio of dsDNA substrate over Cas12a, rather than the absolute dsDNA concentration, was kept constant. Under this condition, the fluorescence increased with the increasing amount of Cas12a and dsDNA (Figure S2D). These results suggested that excess Cas12a could inhibit CALIBURN fluorescence given limited dsDNA substrate. It was noted that the three Cas12a protein preparations exhibited similar performance with the above assays. Based on these results, all the subsequent CALIBURN experiments were performed with 0.05 units of Cas12a and monitored over a course of 120 min.

Screening RT-RPA Primers and crRNA Probes for SARS-CoV-2 Detection. Because the subgenomic RNA

https://dx.doi.org/10.1021/acschembio.0c00840
ACS Chem. Biol. XXXX, XXX, XXX−XXX

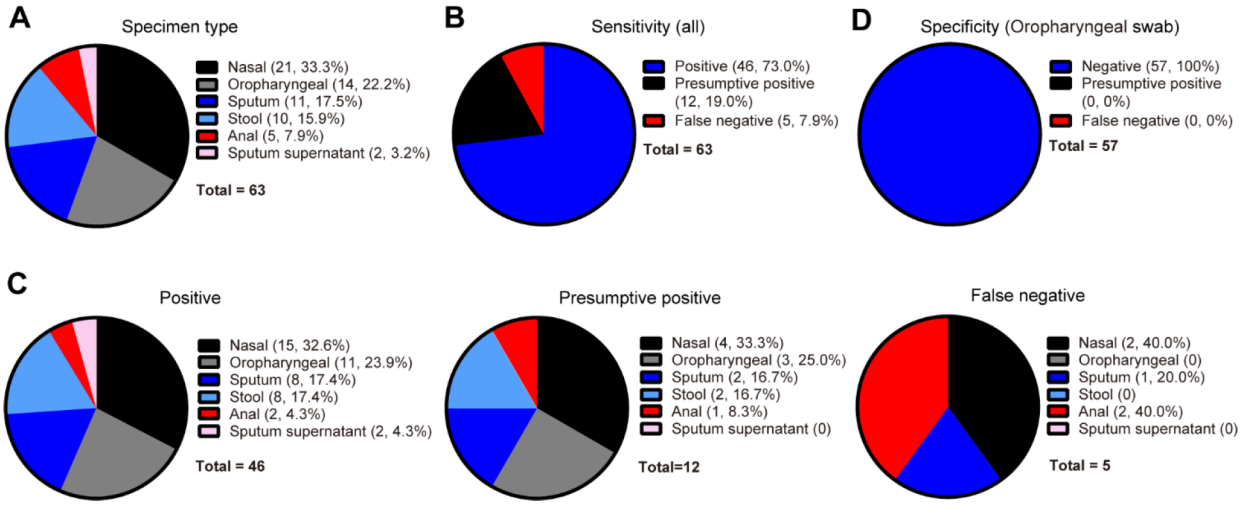

Figure 3. Sensitivity and specificity of CALIBURN for SARS-CoV-2 detection. (A) Types of specimens. (B) Sensitivity of CALIBURN. Positive groups are defined as those with all three CALIBURN replicates reporting a positive signal. Presumptive positive groups are defined as those with one or two CALIBURN replicates reporting a positive signal. False negative groups are defined as those with no CALIBURN replicates reporting a positive signal. (C) Composition of specimen types in the positive, presumptive positive, and false negative groups. (D) Specificity of CALIBURN. The RT-RPA primers and crRNA probes for SARS-CoV-2 are identical to those in Figure 1.

profile of SARS-CoV-2 is complex,[45] we screened RT-RPA primers for ORF1ab, S, E, M, and N genes to identify genomic sites that could be efficiently reverse transcribed and amplified into dsDNA for Cas12a targeting. For each gene target, we designed four forward and four reverse primers and examined all 16 combinations for RT-RPA reaction (Figure S3A and Table S1). Importantly, the RT-RPA products of each gene target were quantified by CALIBURN using a constant crRNA such that the efficiency of RT-RPA primers could be directly coupled with CALIBURN signal readout. It was found that different primer combinations exhibited distinct efficiencies across different gene targets or within each gene target (Figure S3B). It was noted that for certain gene targets such as gene N all primer combinations resulted in relatively high fluorescence signal, while other gene targets such as S and M contained only a couple of primer combinations that yielded a strong fluorescence signal (Figure S3B).

To screen for optimum crRNA for SARS-CoV-2 detection, each gene target was amplified with the RT-RPA primers as described above and then subjected to CALIBURN with different crRNA probes. Four crRNA probes were designed and examined for each site. Similar to the RT-RPA primers, these probes exhibited distinct efficiencies across different gene targets or within each gene target (Figure S4A). Likewise, screening on influenza A virus (IAV) M gene (Figure S4B) and influenza B viruses (IBV) HA gene (Figure S4C) identified optimum crRNA sequences. Interestingly, it was found that IBV crRNA3 could specifically detect Yamagata strain of IBV (Figure S4C).

Specific and Sensitive Detection of Coronaviruses and Influenza Viruses Using CALIBURN. In order to investigate the specificity of CALIBURN, we collected the nucleic acid samples of a series of laboratory strains of coronaviruses and influenza viruses. It was found that the SARS-CoV-2 probe specifically detected SARS-CoV-2 nucleic acids but not other coronaviruses or influenza viruses (Figure 1A). A universal IAV crRNA probe discriminated IAV strains H1N1, H3N2, and H9N2 from coronaviruses and IBVs (Figure 1A). Similarly, IBV strains Yamagata and Victoria could be detected by a universal IBV crRNA probe (Figure 1B). Notably, the optimum combinations of RT-RPA primers and crRNA probes for SARS-CoV-2, IAV, and IBV resulted in fluorescence of comparable level.

We next determined the limit of detection (LOD), defined by the lowest input viral copies resulting in positive signal readouts with more than 95% confidence, of CALIBURN in comparison with reverse transcription PCR (RT-PCR). It was found that the LODs of RT-PCR on the selected gene targets of SARS-CoV-2, IAV, or IBV were in the range 3−12 viral copies per reaction (Figure 2A). In contrast, CALIBURN exhibited LODs of less than 5 viral copies per reaction for the examined viruses (Figure 2B), by comparing the signals under each condition to the threshold of positive signal which was equivalent to the mean plus 3-fold standard deviation (mean $+3\sigma$) of the mock sample. In addition, it was found that fluorescent RT-RPA, without coupled CALIBURN reaction, could detect SARS-CoV-2 with viral copies of 15 or above (Figure 2C). Despite a limited number of tested gene targets, our results indicated that CALIBURN could be leveraged to achieve a sensitivity similar to the conventional RT-PCR or RT-RPA. Importantly, the similar LODs of CALIBURN on detecting SARS-CoV-2, IAV, and IBV could minimize false negative reports that resulted from the differential sensitivity.

CALIBURN Detection of Respiratory Pathogens in Respiratory and Nonrespiratory Specimens. To investigate the compatibility of CALIBURN with different specimen types, we collected 63 SARS-CoV-2 specimens from 6 different forms of preparations including nasal swab, oropharyngeal swab, anal swab, sputum, stool, and sputum supernatant (Figure 3A). The nucleic acid samples were subjected to CALIBURN as described above. For interpretation of the results, the background fluorescence of CALIBURN was subtracted from each sample, and the calibrated data were normalized to that of the mock group, which contains the nucleic acid samples from SARS-CoV-2-negative patients. The threshold for positive signals was set as the mean value plus 3-fold standard deviation (mean$+3\sigma$) of the mock. Under these criteria, CALIBURN reported 73.0% (46/63) positive, 19.0%

https://dx.doi.org/10.1021/acschembio.0c00840
ACS Chem. Biol. XXXX, XXX, XXX−XXX

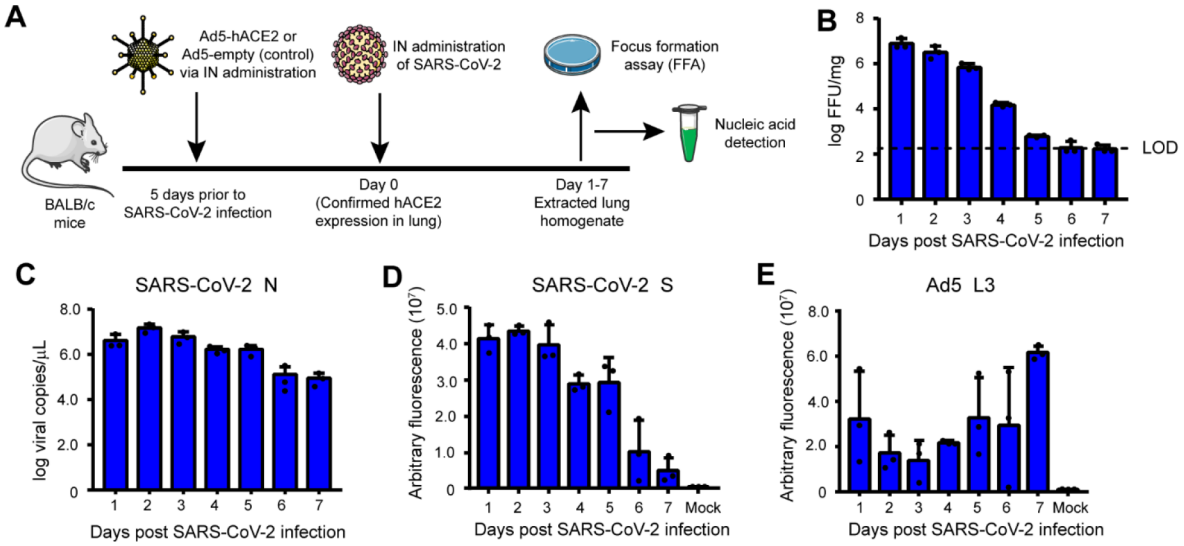

Figure 4. CALIBURN detection of multiple pathogens in SARS-CoV-2 mouse model. (A) Flowchart showing experimental design. (B) Focus forming assay to determine SARS-CoV-2 titers at different time points. LOD, limit of detection. (C) RT-PCR quantification of SARS-CoV-2 viral loads. (D,E) CALIBURN detection of SARS-CoV-2 (D) and Ad5 transcript (E). For the data in C−E, the results from three biological replicates of infection are shown as mean ± SD (n = 3). Each data point represents the mean value of three replicates of detection. The RT-RPA primers and crRNA probes for SARS-CoV-2 are identical to those in Figure 1.

(12/63) presumptive positive where one or two replicates of the samples were above the threshold, and 7.9% (5/63) false negative rates (Figure 3B and Figure S5A). This result is generally consistent with that in a previous study of Cas12a-based SARS-CoV-2 detection.[42] In comparison, conventional RT-PCR reported 92.1% positive and 7.9% presumptive positive rates (Figure S5B). The fluorescence signal of CALIBURN was found to be negatively correlated with the C_t values of RT-PCR (Figure S5A,B). Importantly, a considerable fraction of the samples with low viral loads, as defined by C_t values of greater than 35, could be accurately diagnosed as presumptive positive (Figure S5A,B). By contrast, previous CRISPR detection studies reported very limited number of cases on SARS-CoV-2 samples with high C_t values.[42]

Further analyses of the positive, presumptive positive, and false negative groups as reported by CALIBURN revealed that the compositions of specimen types in the positive and presumptive positive groups (Figure 3C) were generally consistent with the overall composition of specimen types (Figure 3A). This indicated that specimen types did not have a major impact on the outcome of CALIBURN though tests on more specimens were necessary to draw a thorough conclusion. To determine the specificity of CALIBURN, we examined 57 oropharyngeal samples from SARS-CoV-2-negative donors and found that none was tested positive by CALIBURN, thus defining a specificity of 100% (Figure 3D and Figure S5C). Similar to the results with SARS-CoV-2, CALIBURN could detect IAV or IBV in oropharyngeal specimens collected from IAV- or IBV-confirmed patients, respectively (Figure S6A,B).

Detection of Coexisting Pathogens in SARS-CoV-2 Mouse Model. It has been reported that SARS-CoV-2 patients could be coinfected with other respiratory pathogens.[8] Due to the limited clinical samples with coexisting pathogens, we used a recently described SARS-CoV-2 mouse model[46] to evaluate CALIBURN for the parallel detection of multiple pathogens in a single tissue specimen. In this model, an engineered adenovirus serotype 5 (Ad5) carrying human angiotensin-converting enzyme 2 (hACE2) was intranasally administrated to BALB/c mice to support the following SARS-CoV-2 infection. At day 5 post Ad5-hACE2 infection, SARS-CoV-2 was intranasally administrated. Mouse lung tissues were collected at day 1 to day 7 after SARS-CoV-2 infection and then homogenized (Figure 4A). Live SARS-CoV-2 in the lung homogenate was quantified using focus formation assay (Figure 4B), and it was found that the viral loads decreased during the monitored time course (Figure 4B). Viral RNA was extracted from lung homogenate to detect SARS-CoV-2 genome RNA and Ad5 RNA transcripts. RT-PCR suggested a peak of SARS-CoV-2 viral loads at day 2 post-inoculation (Figure 4C). CALIBURN detection revealed time-dependent SARS-CoV-2 viral loads that resembled those of FFU scores and RT-PCR quantification (Figure 4D). To detect Ad5 RNA transcript, we designed several crRNA targeted to the viral capsid protein-encoding gene L3 and identified that crRNA2 exhibited optimum efficiency (Figure S7). CALIBURN detection of Ad5 in the lung homogenate revealed a persistent presence of L3 transcripts with notable variations between samples within the same time points (Figure 4e). These results collectively demonstrated that CALIBURN could sensitively and specifically detect SARS-CoV-2 and Ad5 in parallel.

DISCUSSION

The emerging CRISPR-based nucleic acid diagnostics have many advantages over conventional technologies, including mild reaction conditions, rapid turnover time, single-nucleotide resolution, and broad compatibility with downstream signal readout. These advantages render CRISPR diagnostics the ideal choice for point-of-care testing (POCT) of infectious diseases. In the case of COVID-19, the pandemic has caused a rapidly increasing burden to the conventional clinical diagnostic laboratories. POCT using CRISPR diagnostics may provide a compelling solution to the unmet medical need and help establish airport, community, or even home-based diagnostic strategies for COVID-19.

https://dx.doi.org/10.1021/acschembio.0c00840
ACS Chem. Biol. XXXX, XXX, XXX−XXX

CRISPR-based detection of SARS-CoV-2 has been shown in several proof-of-concept studies.[41−43,47] These studies, however, reported very few cases of detection of SARS-CoV-2 samples with high C_t values. This limitation hampers the widespread application of the CRISPR detection platforms on COVID-19 diagnosis. In the present study, we developed a streamlined nucleic acid detection platform CALIBURN. Unlike other CRISPR detection reaction, the amount of Cas nuclease in the CALIBURN reaction is determined using active units of the proteins. Additionally, we found that excess Cas12a protein over dsDNA substrate could compromise the detection efficiency of CALIBURN. These results suggest that purification of highly active Cas12a proteins is critical to the success of CALIBURN detection. Despite the unclear mechanism of inhibited CALIBURN signal, this observation also indicates that the same formulation of CALIBURN may have drastic performance in detecting clinical samples with high and low viral loads. Importantly, under optimized reaction conditions CALIBURN could successfully detect a large fraction of specimens with low viral loads, thus paving the way to the clinical applications of CRISPR-based pathogen diagnosis.

Another interesting finding was that RT-RPA primers and crRNA probes had unexpectedly large variations in generating a CALIBURN signal. These variations could result from the intrinsic difference in the amplification efficiency of primers or substrate binding efficiency of crRNA. The poorly understood relationship between RT-RPA primer or crRNA sequences and detection efficiency requires that the optimal sequences must be experimentally determined. Importantly, in the current study we identified optimal RT-RPA primers by determining the amplification product that yields maximum CALIBURN fluorescence signal. It has to be noted that the RT-RPA primers and crRNA probes in the present study do not reflect an exhaustive list, and more thorough analyses may be required for commercialization purposes. Engineered Cas variants with altered or broadened protospacer adjacent motif (PAM) sequences may also facilitate the design of RT-RPA primers and crRNA probes.

Furthermore, another advantage of the present study over previous studies lies in the comparative analyses of CALIBURN for detecting SARS-CoV-2 and influenza viruses. We showed that CALIBURN could be leveraged to discriminate SARS-CoV-2, IAV, and IBV from each other and even between the subtypes within each virus. Importantly, unlike previous studies that were primarily focused on SARS-CoV-2, we showed herein that CALIBURN could sensitively detect not only SARS-CoV-2 but also IAV and IBV with LODs similar to or better than conventional RT-PCR. The finding that CALIBURN exhibited LODs of single-digit viral copies for all examined pathogens is critical for the clinical applications of CALIBURN when parallel diagnosis of respiratory viruses is needed. Under clinical settings, CALIBURN can be combined with fluorescence-enabling POCT device or lateral flow[31] for field visualization. In addition, by using the threshold fluorescence signal as reference, CALIBURN allowed quantitative or semiquantitative detection of each pathogen, thus avoiding high rates of false positive or false negative reports. It has been documented that a recently approved CRISPR detection kit with FDA emergency use authorization (EUA) adapts a similar strategy of threshold signal.[48]

Most importantly, our study investigated the effects of specimen types on detection and concluded that CALIBURN was broadly compatible with specimens from different preparations. The FDA EUA CRISPR kit is designed to detect SARS-CoV-2 in upper respiratory specimens.[49] Our results suggest that it would be appropriate to extend the use of CRISPR diagnosis to other specimen types including non-respiratory specimens. However, it must be cautioned that different types of specimens may have distinct viral loads that can affect the diagnostic outcome. One unaddressed issue in our study is the procedure of nucleic acid extraction. It remains unclear whether different reagents or procedures during nucleic acid extraction could affect the detection efficiency of CALIBURN.

It has been known that SARS-CoV-2 infection in human can occur simultaneously with other respiratory viruses such as influenza viruses. To examine whether CALIBURN could be leveraged for the parallel detection of multiple pathogens in a single specimen, we adopted a reported SARS-CoV-2 mouse model where SARS-CoV-2 infection was enabled by the expression of Ad5-delivered ACE2 protein. The genome of Ad5 persists in host cells and is actively transcribed into viral RNA.[50,51] Indeed, we showed that CALIBURN could readily detect both the RNA transcript of Ad5 and the genomic RNA of SARS-CoV-2 in the mouse lung tissues. The consistent results of FFA, RT-PCR, and CALIBURN for SARS-CoV-2 quantification highlight the potential of CALIBURN as a viable technology for monitoring the *in vivo* dynamics of SARS-CoV-2. To the best of our knowledge, our study represents the first CRISPR-based detection of SARS-CoV-2 infection in an animal model.

METHODS

Collection of Samples and Ethics Statement. A total of 63 SARS-CoV-2 samples including nasal swab, oropharyngeal swab, anal swab, sputum, stool, and sputum supernatant specimens were obtained from 18 laboratory-confirmed COVID-19 patients during hospitalization. SARS-CoV-2 samples were collected by The First Affiliated Hospital of Guangzhou Medical University with the consent from patients and approved by the Ethics Committee of the hospital. IAV, IBV and negative samples were collected by Ruijin Hospital with approval from the Ethics Committees of Ruijin Hospital. The project design was approved by the Ethics Committees of ShanghaiTech University.

Preparation of Clinical Samples. SARS-CoV-2 samples were prepared as follows. For nasal, oropharyngeal, and anal swabs, 3 mL of viral transport medium (DMEM containing 2% bovine serum albumin, 15 μg/mL amphotericin, 100 units/mL penicillin G, and 100 μg/mL streptomycin) was added to each collection tube, then vortexed at 2500 rpm for 15 to 30 s, kept at RT for 15 to 30 min, and the supernatant collected. For stool specimens, an equal volume of viral transport medium was added into each tube, then vortexed at 2500 rpm for 15 to 30 s, and the supernatant collected. For sputum supernatant specimens, 1 to 4 volumes of phosphate buffered saline with 0.25 mM ethylenediaminetetraacetic acid (EDTA) was added to each tube, then vortexed at 2500 rpm for 15 to 30 s, and the supernatant collected. For sputum specimens, an equal volume of 2% dithiothreitol (DTT) was added to the sputum precipitates, then vortexed at 2500 rpm for 15 to 30 s, and the supernatant collected. All the supernatant was transferred to lysis buffer for RNA extraction. IAV, IBV, and negative samples were extracted using TIANamp Virus DNA/RNA Kit (DP315, TIANGEN, Beijing, China) according to the manufacturer's instructions. The mock samples used for each pathogen were collected from patients free of the corresponding pathogens that contained relatively high concentration of nucleic acids, which were expected to give a high level of nonspecific signals.

Expression and Purification of Cas12a. The expression and purification of Cas12a were performed as previously described with

https://dx.doi.org/10.1021/acschembio.0c00840
ACS Chem. Biol. XXXX, XXX, XXX−XXX

modifications. Codon optimized gene encoding Cas12a protein from *Lachnospiraceae bacterium* ND2006 (LbCas12a) was cloned into pET28a vector to enable inducible protein expression under the control of T7 promoter. A 6 × His-tag was added to the C-terminus of LbCas12a with a TEV protease cleavage site inserted in between. The recombinant plasmid, referred to as pET28a-LbCas12a, was transformed into *Escherichia coli* BL21 (DE3). The next day a single colony was picked and cultured in Luria−Bertani (LB) broth supplemented with 50 μg/mL kanamycin at 37 °C with shaking. At an OD_{600} of 0.8, 1 mM isopropyl β-D-1-thiogalactopyranoside (IPTG) was added into the culture and protein expression was induced at 37 °C for 4 h. Cells were harvested by centrifugation at 5000 *g* for 10 min at 4 °C.

Collected cells are resuspended in lysis buffer containing 20 mM Tris-HCl, pH 8.0, 500 mM NaCl, 10% (v/v) glycerol, and 0.5 mM phenylmethylsulfonyl fluoride (PMSF). Expressed Cas12a protein was purified using Ni-NTA resin (Qiagen, Shanghai, China). Further purification was performed using fast protein liquid chromatography (FPLC) with Superdex200 filtration column (GE Healthcare Life Sciences, Connecticut, USA). Purified proteins were concentrated, exchanged to storage buffer containing 20 mM Tris-HCl, pH 7.5, 500 mM NaCl, 10% (v/v) glycerol, and 2 mM dithiolthreitol (DTT); aliquoted; and stored at −80 °C. Protein concentration was determined using BCA Protein Assay Kit (Thermo Fisher Scientific, Massachusetts, USA).

Preparation of crRNA and DNA Substrate. crRNA probes were synthesized by GenScript Biotech (Nanjing, Jiangsu, China). The DNA encoding the ORF1ab gene of SARS-CoV-2, M gene of IAV, and HA gene of IBV was synthesized by TSINGKE Biological Technology (Shanghai, China) and cloned into a pUC57 vector. The DNA substrate of Cas12a was prepared by PCR amplification using RT-RPA primers.

Isothermal Amplification. Isothermal amplification was performed using a commercial RT-RPA kit (Qitian Gene Biotech, Wuxi, Jiangsu, China) according to the manufacturer's instructions. Briefly, a 50 μL reaction containing 20 mM Tris-HCl, pH 7.0, 200 mM sodium acetate, 10 mM DTT, 10 mM adenosine triphosphate, 500 μM deoxyribonucleoside triphosphate, 10 mM creatine phosphate disodium salt, 100 mM creatine kinase, 10% (v/v) trehalose, 50 ng/L mannitol, 200 ng/μL single-stranded DNA-binding protein, 500 ng/μL recombinase RecA, 400 ng/μL DNA polymerase, 20 U reverse transcriptase, 4% (v/v) polyethylene glycol, 5 μL laboratory or clinical samples, 0.4 μM each of forward and reverse RT-RPA primers (Table S2), and 14 mM magnesium acetate was incubated at 42 °C for 30 min. Fluorescent RT-RPA was performed as described above with an additional 50 ng/μL exonuclease, and the products were detected with 50 nM Taqman probe (Table S2). The signal of fluorescent RT-RPA was detected by SpectraMax iD3Multi-Mode Microplate Reader (Molecular Devices, San Jose, USA) with an excitation wavelength of 485 nm and an emission wavelength of 520 nm.

RT-PCR. RNA samples of 2 μL were used for the reverse transcription reaction using PrimeScript RT reagent Kit (TaKaRa, Japan). PCR primers were designed according to WHO[52] or Chinese CDC's instructions[53] and are listed in Table S3. The RT-PCR was performed in a 10 μL reaction containing 5 μL of PowerUp SYBR Green Master Mix (Applied Biosystems, USA), 0.5 μL of each forward and reverse primers with a stock concentration of 10 μM, and 0.5 μL of reverse transcribed cDNA products. The reaction was incubated on QuantStudio 6 Flex System thermocycler (Applied Biosystems, USA) using the following cycling conditions: 50 °C for 2 min, 95 °C for 2 min, and 40 cycles of 95 °C denaturation for 15 s and 60 °C annealing extension for 1 min. Fluorescence signal was collected at the 60 °C annealing extension step in each cycle.

Cas12a-Linked Beam Unlocking Reaction (CALIBURN). Unless otherwise noted, CALIBURN was performed in a 20 μL reaction containing 50 mM Tris-HCl, pH 7.5, 100 mM NaCl, 10 mM $MgCl_2$, 100 μg/mL bovine serum albumin (BSA), 0.05 unit of purified LbCas12a, 1.25 μM ssDNA-FAM/BQ1 probe (General Biosystems, Chuzhou, Anhui, China), 100 nM crRNA, and 5 μL RT-RPA reaction products or dsDNA substrate of indicated amount. The reaction was incubated at 37 °C and monitored over a course of 120 min. The end points of the reaction for detection applications were set at 30 min unless noted otherwise. The fluorescence signal was detected by SpectraMax iD3Multi-Mode Microplate Reader (Molecular Devices, San Jose, USA) with an excitation wavelength of 485 nm and an emission wavelength of 520 nm.

Mouse Model of SARS-CoV-2. The SARS-CoV-2 virus used in this study was isolated from a COVID-19 patient in Guangzhou (Accession numbers: MT123290) and passaged on African Green monkey kidney-derived Vero E6 cells. Vero E6 cells were grown in Dulbecco's modified Eagle's medium (DMEM; Thermo, Waltham, USA) supplemented with 10% fetal bovine serum (FBS; Thermo, Waltham, USA).

Specific pathogen-free BALB/c mice of 6−8 weeks old were purchased from Hunan SJA Laboratory Animal Co. (Hunan, China) and maintained in the Animal Care Facilities at the Guangzhou Medical University. For SARS-CoV-2 infection model, mice were lightly anesthetized with isoflurane and transduced intranasally with 2.5×10^8 focus forming units (FFU) of human serotype 5 adenoviral vector (Ad5) expressing human ACE2 under the control of the CMV promoter (Ad5-hACE2) or empty Ad5 vector (Ad5-Empty)[50,51] in 75 μL DMEM. At day 5 post Ad5-hACE2 transduction, mice were infected intranasally with 1×10^5 plaque forming units (PFU) of SARS-CoV-2 in a total volume of 50 μL DMEM. Mice were monitored and weighed daily. All work with SARS-CoV-2 was conducted in the Biosafety Level 3 (BSL3) Laboratories of Guangzhou Customs District Technology Center. All protocols were approved by the Institutional Animal Care and Use Committees of the Guangzhou Medical University.

Focus Forming Assay (FFA). SARS-CoV-2 virus was titrated using FFA as a high-throughput assay. Briefly, Vero E6 cells were seeded in 96-well plates 1 day before infection. Virus culture or lung homogenate was serially diluted and used to inoculate Vero E6 cells at 37 °C for 1 h. Virus-containing medium was then removed, and 125 μL of 1.6% prewarmed carboxymethylcellulose was added to each well. After 24 h after inoculation, cells were fixed with 4% paraformaldehyde and permeabilized with 0.2% Triton X-100. Cells were then incubated with a rabbit anti-SARS-CoV-2 nucleocapsid protein polyclonal antibody (Cat. No.: 40143-T62, Sino Biological, Inc. Beijing), followed by an HRP-labeled goat anti-rabbit secondary antibody (Cat. No.: 109-035-088, Jackson ImmunoResearch Laboratories, Inc. West Grove, PA). The foci were visualized by TrueBlue Peroxidase Substrate (KPL, Gaithersburg, MD) and counted with an ELISPOT reader (Cellular Technology Ltd. Cleveland, OH). Viral titers were calculated as FFU per mL or per gram tissue.

Statistical Analyses. All data are the results from at least three biological replicates and are shown as mean ± SD. Statistical analyses were performed with one-way ANOVA with Tukey's multiple comparisons test or two-way ANOVA with Dunnett's multiple comparisons test unless otherwise noted.

■ ASSOCIATED CONTENT

Supporting Information

The Supporting Information is available free of charge at https://pubs.acs.org/doi/10.1021/acschembio.0c00840.

Determination of the active units of purified Cas12a proteins; Analyses of the effects of dsDNA substrate, reaction time, and Cas12a on CALIBURN; Screening RT-RPA primers for SARS-CoV-2 detection; Screening crRNA probes for SARS-CoV-2, IAV, and IBV; Determination of the sensitivity and specificity of CALIBURN using SARS-CoV-2-positive and negative clinical samples, respectively; CALIBURN detection of IAV and IBV specimens; Screening crRNA probes for Ad5 L3 gene; Primers for RT-RPA amplification; crRNA target sites in the amplified dsDNA products of viral

https://dx.doi.org/10.1021/acschembio.0c00840
ACS Chem. Biol. XXXX, XXX, XXX−XXX

genome; RT-PCR primers; Protein sequence of the LbCas12a construct in this study (PDF)

AUTHOR INFORMATION

Corresponding Authors

Xianxing Jiang − *Guangdong Key Laboratory of Chiral Molecule and Drug Discovery, School of Pharmaceutical Sciences, Sun Yat-Sen University, Guangzhou, Guangdong 510006, China;* orcid.org/0000-0002-7508-2368; Email: jiangxx5@mail.sysu.edu.cn

Jieming Qu − *Department of Pulmonary and Critical Care Medicine, Ruijin Hospital and Institutes of Respiratory Diseases, School of Medicine, Shanghai Jiao Tong University, Shanghai 200025, China*; Email: jmqu0906@163.com

Jincun Zhao − *State Key Laboratory of Respiratory Disease, National Clinical Research Center for Respiratory Disease, Guangzhou Institute of Respiratory Health, the First Affiliated Hospital of Guangzhou Medical University, Guangzhou 510182, China*; Email: zhaojincun@gird.cn

Jia Liu − *Shanghai Institute for Advanced Immunochemical Studies, ShanghaiTech University, Shanghai 201210, China; School of Life Science and Technology, ShanghaiTech University, Shanghai 201210, China; State Key Laboratory of Respiratory Disease, National Clinical Research Center for Respiratory Disease, Guangzhou Institute of Respiratory Health, the First Affiliated Hospital of Guangzhou Medical University, Guangzhou 510182, China;* orcid.org/0000-0001-9787-465X; Email: liujia@shanghaitech.edu.cn

Authors

Yu Wang − *Shanghai Institute for Advanced Immunochemical Studies, ShanghaiTech University, Shanghai 201210, China; Guangdong Key Laboratory of Chiral Molecule and Drug Discovery, School of Pharmaceutical Sciences, Sun Yat-Sen University, Guangzhou, Guangdong 510006, China*

Donglan Liu − *State Key Laboratory of Respiratory Disease, National Clinical Research Center for Respiratory Disease, Guangzhou Institute of Respiratory Health, the First Affiliated Hospital of Guangzhou Medical University, Guangzhou 510182, China*

Huihuang Lin − *Department of Pulmonary and Critical Care Medicine, Ruijin Hospital and Institutes of Respiratory Diseases, School of Medicine, Shanghai Jiao Tong University, Shanghai 200025, China*

Dingbin Chen − *State Key Laboratory of Respiratory Disease, National Clinical Research Center for Respiratory Disease, Guangzhou Institute of Respiratory Health, the First Affiliated Hospital of Guangzhou Medical University, Guangzhou 510182, China*

Jing Sun − *State Key Laboratory of Respiratory Disease, National Clinical Research Center for Respiratory Disease, Guangzhou Institute of Respiratory Health, the First Affiliated Hospital of Guangzhou Medical University, Guangzhou 510182, China*

Yusang Xie − *Department of Pulmonary and Critical Care Medicine, Ruijin Hospital and Institutes of Respiratory Diseases, School of Medicine, Shanghai Jiao Tong University, Shanghai 200025, China*

Xinjie Wang − *Shanghai Institute for Advanced Immunochemical Studies, ShanghaiTech University, Shanghai 201210, China*

Peixiang Ma − *Shanghai Institute for Advanced Immunochemical Studies, ShanghaiTech University, Shanghai 201210, China*

Yan Nie − *Shanghai Institute for Advanced Immunochemical Studies, ShanghaiTech University, Shanghai 201210, China;* orcid.org/0000-0003-2521-8519

Hong Mei − *Shanghai Institute for Advanced Immunochemical Studies, ShanghaiTech University, Shanghai 201210, China*

Baihui Zhao − *Shanghai BioGerm Medical Biotechnology Co., Ltd, Shanghai 201318, China*

Xingxu Huang − *School of Life Science and Technology, ShanghaiTech University, Shanghai 201210, China*

Ge Jiang − *Shanghai Institute for Advanced Immunochemical Studies, ShanghaiTech University, Shanghai 201210, China*

Complete contact information is available at: https://pubs.acs.org/10.1021/acschembio.0c00840

Author Contributions

¶J.L., J.Z., J.Q., and X.J. designed the experiments and drafted the manuscript. Y.W., D.L. and H.L. led the projects and carried out the experiments throughout the whole project. D.L. and J.S. performed experiments on SARS-CoV-2 mouse model and collected the nucleic acid samples from mouse lung tissues. B.Z., Y.X., H.M. and G.J. organized or prepared critical resources including clinical or laboratory nucleic acid samples. P.M. and Y.N. prepared Cas12a protein samples. X.W. and X.H. provided technical support. Y.W., D.L., and H.L. contributed equally to this work.

Funding

Zhangjiang National Innovation Demonstration Zone (ZJ2020-ZD-004 to B.Z. and G.J.), Zhejiang University special scientific research fund for COVID-19 prevention and control (2020XGZX011 to J.Q. and J.L.), Cultivation Project of Shanghai Major Infectious Disease Research Base (20dz2210500 to J.Q.), the National Key Research and Development Program of China (2018YFC1200100 and 2018ZX10301403 to J.Z.), the emergency grants for prevention and control of SARS-CoV-2 of Ministry of Science and Technology (2020YFC0841400 to J.Z.), Shanghai Municipal Key Clinical Specialty (shslczdzk02202 to J.Q.), Shanghai Top-Priority Clinical Key Disciplines Construction Project (2017ZZ02014 to J.Q.), Shanghai Shenkang Hospital Development Center Clinical Science and Technology Innovation Project (SHDC12018102 to J.Q.), National Innovative Research Team of High-level Local Universities in Shanghai (to J.Q.), National Natural Science Foundation of China (91853106 to X.J.), the Program for Guangdong Introducing Innovative and Enterpre-neurial Teams (2016ZT06Y337 to X.J.), the Fundamental Research Funds for the Central Universities (19ykzd25 to X.J.), Key Laboratory of Emergency Prevention, Diagnosis and Treatment of Respiratory Infectious Diseases, Shanghai (20dz2261100 to J.Q.), ShanghaiTech University COVID-19 Special Fund (to G.J.), ShanghaiTech University Startup Fund (2019F0301-000-01 to J.L.).

Notes

B.Z. is a cofounder of Shanghai BioGerm Medical Biotechnology Co., Ltd.

https://dx.doi.org/10.1021/acschembio.0c00840
ACS Chem. Biol. XXXX, XXX, XXX−XXX

■ ACKNOWLEDGMENTS

The authors thank the High-Throughput Screening Platform at Shanghai Institute for Advanced Immunochemical Studies (SIAIS) at ShanghaiTech University for the support of CALIBURN experiments.

■ REFERENCES

(1) Zhu, N., Zhang, D., Wang, W., Li, X., Yang, B., Song, J., Zhao, X., Huang, B., Shi, W., Lu, R., Niu, P., Zhan, F., Ma, X., Wang, D., Xu, W., Wu, G., Gao, G. F., and Tan, W. (2020) A novel coronavirus from patients with pneumonia in China, 2019. *N. Engl. J. Med. 382*, 727−733.

(2) Wu, F., Zhao, S., Yu, B., Chen, Y. M., Wang, W., Song, Z. G., Hu, Y., Tao, Z. W., Tian, J. H., Pei, Y. Y., Yuan, M. L., Zhang, Y. L., Dai, F. H., Liu, Y., Wang, Q. M., Zheng, J. J., Xu, L., Holmes, E. C., and Zhang, Y. Z. (2020) A new coronavirus associated with human respiratory disease in China. *Nature 579*, 265−269.

(3) WHO. (2020) Coronavirus disease (COVID-19) situation dashboard, January 06, 2021. *WHO webpage*; https://www.who.int.

(4) Lauer, S. A., Grantz, K. H., Bi, Q., Jones, F. K., Zheng, Q., Meredith, H. R., Azman, A. S., Reich, N. G., and Lessler, J. (2020) The incubation period of coronavirus disease 2019 (COVID-19) from publicly reported confirmed cases: estimation and application. *Ann. Intern. Med. 172*, 577−582.

(5) Guan, W. J., Ni, Z. Y., Hu, Y., Liang, W. H., Ou, C. Q., He, J. X., Liu, L., Shan, H., Lei, C. L., Hui, D. S. C., Du, B., Li, L. J., Zeng, G., Yuen, K. Y., Chen, R. C., Tang, C. L., Wang, T., Chen, P. Y., Xiang, J., Li, S. Y., Wang, J. L., Liang, Z. J., Peng, Y. X., Wei, L., Liu, Y., Hu, Y. H., Peng, P., Wang, J. M., Liu, J. Y., Chen, Z., Li, G., Zheng, Z. J., Qiu, S. Q., Luo, J., Ye, C. J., Zhu, S. Y., and Zhong, N. S. (2020) Clinical characteristics of coronavirus disease 2019 in China. *N. Engl. J. Med. 382*, 1708−1720.

(6) Chen, N., Zhou, M., Dong, X., Qu, J., Gong, F., Han, Y., Qiu, Y., Wang, J., Liu, Y., Wei, Y., Xia, J., Yu, T., Zhang, X., and Zhang, L. (2020) Epidemiological and clinical characteristics of 99 cases of 2019 novel coronavirus pneumonia in Wuhan, China: a descriptive study. *Lancet 395*, 507−513.

(7) Kong, W. H., Li, Y., Peng, M. W., Kong, D. G., Yang, X. B., Wang, L., and Liu, M. Q. (2020) SARS-CoV-2 detection in patients with influenza-like illness. *Nat. Microbiol. 5*, 675−678.

(8) Wu, X., Cai, Y., Huang, X., Yu, X., Zhao, L., Wang, F., Li, Q., Gu, S., Xu, T., Li, Y., Lu, B., and Zhan, Q. (2020) Co-infection with SARS-CoV-2 and influenza A virus in patient with pneumonia, China. *Emerging Infect. Dis. 26*, 1324−1326.

(9) Zhou, P., Yang, X. L., Wang, X. G., Hu, B., Zhang, L., Zhang, W., Si, H. R., Zhu, Y., Li, B., Huang, C. L., Chen, H. D., Chen, J., Luo, Y., Guo, H., Jiang, R. D., Liu, M. Q., Chen, Y., Shen, X. R., Wang, X., Zheng, X. S., Zhao, K., Chen, Q. J., Deng, F., Liu, L. L., Yan, B., Zhan, F. X., Wang, Y. Y., Xiao, G. F., and Shi, Z. L. (2020) A pneumonia outbreak associated with a new coronavirus of probable bat origin. *Nature 579*, 270−273.

(10) Cui, J., Li, F., and Shi, Z. L. (2019) Origin and evolution of pathogenic coronaviruses. *Nat. Rev. Microbiol. 17*, 181−192.

(11) Chan, J. F., Kok, K. H., Zhu, Z., Chu, H., To, K. K., Yuan, S., and Yuen, K. Y. (2020) Genomic characterization of the 2019 novel human-pathogenic coronavirus isolated from a patient with atypical pneumonia after visiting Wuhan. *Emerging Microbes Infect. 9*, 221−236.

(12) Lu, R., Zhao, X., Li, J., Niu, P., Yang, B., Wu, H., Wang, W., Song, H., Huang, B., Zhu, N., Bi, Y., Ma, X., Zhan, F., Wang, L., Hu, T., Zhou, H., Hu, Z., Zhou, W., Zhao, L., Chen, J., Meng, Y., Wang, J., Lin, Y., Yuan, J., Xie, Z., Ma, J., Liu, W. J., Wang, D., Xu, W., Holmes, E. C., Gao, G. F., Wu, G., Chen, W., Shi, W., and Tan, W. (2020) Genomic characterisation and epidemiology of 2019 novel coronavirus: implications for virus origins and receptor binding. *Lancet 395*, 565−574.

(13) Corman, V. M., Landt, O., Kaiser, M., Molenkamp, R., Meijer, A., Chu, D. K., Bleicker, T., Brunink, S., Schneider, J., Schmidt, M. L., Mulders, D. G., Haagmans, B. L., van der Veer, B., van den Brink, S., Wijsman, L., Goderski, G., Romette, J. L., Ellis, J., Zambon, M., Peiris, M., Goossens, H., Reusken, C., Koopmans, M. P., and Drosten, C. (2020) Detection of 2019 novel coronavirus (2019-nCoV) by real-time RT-PCR. *Euro Surveill. 25*, 2000045.

(14) Chu, D. K. W., Pan, Y., Cheng, S. M. S., Hui, K. P. Y., Krishnan, P., Liu, Y., Ng, D. Y. M., Wan, C. K. C., Yang, P., Wang, Q., Peiris, M., and Poon, L. L. M. (2020) Molecular diagnosis of a novel coronavirus (2019-nCoV) causing an outbreak of pneumonia. *Clin. Chem. 66*, 549−555.

(15) Yu, F., Yan, L., Wang, N., Yang, S., Wang, L., Tang, Y., Gao, G., Wang, S., Ma, C., Xie, R., Wang, F., Tan, C., Zhu, L., Guo, Y., and Zhang, F. (2020) Quantitative detection and viral load analysis of SARS-CoV-2 in infected patients. *Clin. Infect. Dis. 71*, 793−798.

(16) Wang, X., Yao, H., Xu, X., Zhang, P., Zhang, M., Shao, J., Xiao, Y., and Wang, H. (2020) Limits of detection of six approved RT-PCR kits for the novel SARS-coronavirus-2 (SARS-CoV-2). *Clin. Chem. 66*, 977−979.

(17) Pfefferle, S., Reucher, S., Norz, D., and Lutgehetmann, M. (2020) Evaluation of a quantitative RT-PCR assay for the detection of the emerging coronavirus SARS-CoV-2 using a high throughput system. *Euro Surveill. 25*, 2000152.

(18) Yelin, I., Aharony, N., Shaer Tamar, E., Argoetti, A., Messer, E., Berenbaum, D., Shafran, E., Kuzli, A., Gandali, N., Shkedi, O., Hashimshony, T., Mandel-Gutfreund, Y., Halberthal, M., Geffen, Y., Szwarcwort-Cohen, M., and Kishony, R. (2020) Evaluation of COVID-19 RT-qPCR test in multi-sample pools. *Clin. Infect. Dis. 71*, 2073.

(19) East-Seletsky, A., O'Connell, M. R., Knight, S. C., Burstein, D., Cate, J. H., Tjian, R., and Doudna, J. A. (2016) Two distinct RNase activities of CRISPR-C2c2 enable guide-RNA processing and RNA detection. *Nature 538*, 270−273.

(20) Gootenberg, J. S., Abudayyeh, O. O., Lee, J. W., Essletzbichler, P., Dy, A. J., Joung, J., Verdine, V., Donghia, N., Daringer, N. M., Freije, C. A., Myhrvold, C., Bhattacharyya, R. P., Livny, J., Regev, A., Koonin, E. V., Hung, D. T., Sabeti, P. C., Collins, J. J., and Zhang, F. (2017) Nucleic acid detection with CRISPR-Cas13a/C2c2. *Science 356*, 438−442.

(21) Barrangou, R., Fremaux, C., Deveau, H., Richards, M., Boyaval, P., Moineau, S., Romero, D. A., and Horvath, P. (2007) CRISPR provides acquired resistance against viruses in prokaryotes. *Science 315*, 1709−1712.

(22) Brouns, S. J., Jore, M. M., Lundgren, M., Westra, E. R., Slijkhuis, R. J., Snijders, A. P., Dickman, M. J., Makarova, K. S., Koonin, E. V., and van der Oost, J. (2008) Small CRISPR RNAs guide antiviral defense in prokaryotes. *Science 321*, 960−964.

(23) Marraffini, L. A., and Sontheimer, E. J. (2008) CRISPR interference limits horizontal gene transfer in staphylococci by targeting DNA. *Science 322*, 1843−1845.

(24) Jinek, M., East, A., Cheng, A., Lin, S., Ma, E., and Doudna, J. (2013) RNA-programmed genome editing in human cells. *eLife 2*, e00471.

(25) Mali, P., Yang, L., Esvelt, K. M., Aach, J., Guell, M., DiCarlo, J. E., Norville, J. E., and Church, G. M. (2013) RNA-guided human genome engineering via Cas9. *Science 339*, 823−826.

(26) Cong, L., Ran, F. A., Cox, D., Lin, S., Barretto, R., Habib, N., Hsu, P. D., Wu, X., Jiang, W., Marraffini, L. A., and Zhang, F. (2013) Multiplex genome engineering using CRISPR/Cas systems. *Science 339*, 819−823.

(27) Cho, S. W., Kim, S., Kim, J. M., and Kim, J. S. (2013) Targeted genome engineering in human cells with the Cas9 RNA-guided endonuclease. *Nat. Biotechnol. 31*, 230−232.

(28) Pickar-Oliver, A., and Gersbach, C. A. (2019) The next generation of CRISPR-Cas technologies and applications. *Nat. Rev. Mol. Cell Biol. 20*, 490−507.

(29) Myhrvold, C., Freije, C. A., Gootenberg, J. S., Abudayyeh, O. O., Metsky, H. C., Durbin, A. F., Kellner, M. J., Tan, A. L., Paul, L. M., Parham, L. A., Garcia, K. F., Barnes, K. G., Chak, B., Mondini, A., Nogueira, M. L., Isern, S., Michael, S. F., Lorenzana, I., Yozwiak, N. L.,

https://dx.doi.org/10.1021/acschembio.0c00840
ACS Chem. Biol. XXXX, XXX, XXX−XXX

MacInnis, B. L., Bosch, I., Gehrke, L., Zhang, F., and Sabeti, P. C. (2018) Field-deployable viral diagnostics using CRISPR-Cas13. *Science 360*, 444−448.
(30) Chen, J. S., Ma, E., Harrington, L. B., Da Costa, M., Tian, X., Palefsky, J. M., and Doudna, J. A. (2018) CRISPR-Cas12a target binding unleashes indiscriminate single-stranded DNase activity. *Science 360*, 436−439.
(31) Gootenberg, J. S., Abudayyeh, O. O., Kellner, M. J., Joung, J., Collins, J. J., and Zhang, F. (2018) Multiplexed and portable nucleic acid detection platform with Cas13, Cas12a, and Csm6. *Science 360*, 439−444.
(32) Teng, F., Guo, L., Cui, T., Wang, X. G., Xu, K., Gao, Q., Zhou, Q., and Li, W. (2019) CDetection: CRISPR-Cas12b-based DNA detection with sub-attomolar sensitivity and single-base specificity. *Genome Biol. 20*, 132.
(33) Dai, Y., Somoza, R. A., Wang, L., Welter, J. F., Li, Y., Caplan, A. I., and Liu, C. C. (2019) Exploring the trans-cleavage activity of CRISPR-Cas12a (cpf1) for the development of a universal electrochemical biosensor. *Angew. Chem., Int. Ed. 58*, 17399−17405.
(34) Mukama, O., Wu, J., Li, Z., Liang, Q., Yi, Z., Lu, X., Liu, Y., Hussain, M., Makafe, G. G., Liu, J., Xu, N., and Zeng, L. (2020) An ultrasensitive and specific point-of-care CRISPR/Cas12 based lateral flow biosensor for the rapid detection of nucleic acids. *Biosens. Bioelectron. 159*, 112143.
(35) Liang, M., Li, Z., Wang, W., Liu, J., Liu, L., Zhu, G., Karthik, L., Wang, M., Wang, K. F., Wang, Z., Yu, J., Shuai, Y., Zhang, L., Yang, Z., Li, C., Zhang, Q., Shi, T., Zhou, L., Xie, F., Dai, H., Liu, X., Zhang, J., Liu, G., Zhuo, Y., Zhang, B., Liu, C., Li, S., Xia, X., Tong, Y., Liu, Y., Alterovitz, G., Tan, G. Y., and Zhang, L. X. (2019) A CRISPR-Cas12a-derived biosensing platform for the highly sensitive detection of diverse small molecules. *Nat. Commun. 10*, 3672.
(36) Xiong, Y., Zhang, J., Yang, Z., Mou, Q., Ma, Y., and Lu, Y. (2020) Functional DNA regulated CRISPR-Cas12a sensors for point-of-care diagnostics of non-nucleic-acid targets. *J. Am. Chem. Soc. 142*, 207−213.
(37) Bai, J., Lin, H., Li, H., Zhou, Y., Liu, J., Zhong, G., Wu, L., Jiang, W., Du, H., Yang, J., Xie, Q., and Huang, L. (2019) Cas12a-based on-site and rapid nucleic acid detection of African Swine Fever. *Front. Microbiol. 10*, 2830.
(38) Yuan, C., Tian, T., Sun, J., Hu, M., Wang, X., Xiong, E., Cheng, M., Bao, Y., Lin, W., Jiang, J., Yang, C., Chen, Q., Zhang, H., Wang, H., Deng, X., Liao, X., Liu, Y., Wang, Z., Zhang, G., and Zhou, X. (2020) Universal and naked-eye gene detection platform based on the clustered regularly interspaced short palindromic repeats/Cas12a/13a system. *Anal. Chem. 92*, 4029−4037.
(39) Wang, X., Ji, P., Fan, H., Dang, L., Wan, W., Liu, S., Li, Y., Yu, W., Li, X., Ma, X., Zhao, Q., Huang, X., and Liao, M. (2020) CRISPR/Cas12a technology combined with immunochromatographic strips for portable detection of African swine fever virus. *Commun. Biol. 3*, 62.
(40) He, Q., Yu, D., Bao, M., Korensky, G., Chen, J., Shin, M., Kim, J., Park, M., Qin, P., and Du, K. (2020) High-throughput and all-solution phase African Swine Fever Virus (ASFV) detection using CRISPR-Cas12a and fluorescence based point-of-care system. *Biosens. Bioelectron. 154*, 112068.
(41) Wang, X. J., Zhong, M. T., Liu, Y., Ma, P. X., Dang, L., Meng, Q. Z., Wan, W. W., Ma, X. D., Liu, J., Yang, G., Yang, Z. F., Huang, X. X., and Liu, M. (2020) Rapid and sensitive detection of COVID-19 using CRISPR/Cas12a-based detection with naked eye readout, CRISPR/Cas12a-NER. *Sci. Bull. 65*, 1436−1439.
(42) Broughton, J. P., Deng, X. D., Yu, G. X., Fasching, C. L., Servellita, V., Singh, J., Miao, X., Streithorst, J. A., Granados, A., Sotomayor-Gonzalez, A., Zorn, K., Gopez, A., Hsu, E., Gu, W., Miller, S., Pan, C. Y., Guevara, H., Wadford, D. A., Chen, J. S., and Chiu, C. Y. (2020) CRISPR-Cas12-based detection of SARS-CoV-2. *Nat. Biotechnol. 38*, 870−874.
(43) Guo, L., Sun, X., Wang, X., Liang, C., Jiang, H., Gao, Q., Dai, M., Qu, B., Fang, S., Mao, Y., Chen, Y., Feng, G., Gu, Q., Wang, R. R., Zhou, Q., and Li, W. (2020) SARS-CoV-2 detection with CRISPR diagnostics. *Cell Discovery 6*, 34.
(44) Lobato, I. M., and O'Sullivan, C. K. (2018) Recombinase polymerase amplification: Basics, applications and recent advances. *TrAC, Trends Anal. Chem. 98*, 19−35.
(45) Kim, D., Lee, J. Y., Yang, J. S., Kim, J. W., Kim, V. N., and Chang, H. (2020) The architecture of SARS-CoV-2 transcriptome. *Cell 181*, 914.
(46) Sun, J., Zhuang, Z., Zheng, J., Li, K., Wong, R. L. Y., Liu, D. L., Huang, J. C., He, J. P., Zhu, A. R., Zhao, J. X., Li, X. B., Xi, Y., Chen, R. C., Alshukairi, A. N., Chen, Z., Zhang, Z. Y., Chen, C. K., Huang, X. F., Li, F., Lai, X. M., Chen, D. B., Wen, L. Y., Zhuo, J. F., Zhang, Y. J., Wang, Y. Q., Huang, S. X., Dai, J., Shi, Y. X., Zheng, K., Leidinger, M. R., Chen, J. K., Li, Y. M., Zhong, N. S., Meyerholz, D. K., McCray, P. B., Perlman, S., and Zhao, J. C. (2020) Generation of a broadly useful model for COVID-19 pathogenesis, vaccination, and treatment. *Cell 182*, 734−743.
(47) Ackerman, C. M., Myhrvold, C., Thakku, S. G., Freije, C. A., Metsky, H. C., Yang, D. K., Ye, S. H., Boehm, C. K., Kosoko-Thoroddsen, T. S. F., Kehe, J., Nguyen, T. G., Carter, A., Kulesa, A., Barnes, J. R., Dugan, V. G., Hung, D. T., Blainey, P. C., and Sabeti, P. C. (2020) Massively multiplexed nucleic acid detection with Cas13. *Nature 582*, 277−282.
(48) Guglielmi, G. (2020) First CRISPR test for the coronavirus approved in the United States. *Nature*, 1 DOI: 10.1038/d41586-020-01402-9.
(49) SHERLOCK (2020) INSTRUCTIONS FOR USE-Sherlock™ CRISPR SARS-CoV-2 kit. *SHERLOCK Biosciences*.
(50) Luo, J., Deng, Z. L., Luo, X., Tang, N., Song, W. X., Chen, J., Sharff, K. A., Luu, H. H., Haydon, R. C., Kinzler, K. W., Vogelstein, B., and He, T. C. (2007) A protocol for rapid generation of recombinant adenoviruses using the AdEasy system. *Nat. Protoc. 2*, 1236−1247.
(51) Zhao, J., Li, K., Wohlford-Lenane, C., Agnihothram, S. S., Fett, C., Gale, M. J., Jr., Baric, R. S., Enjuanes, L., Gallagher, T., McCray, P. B., Jr., and Perlman, S. (2014) Rapid generation of a mouse model for Middle East respiratory syndrome. *Proc. Natl. Acad. Sci. U. S. A. 111*, 4970−4975.
(52) WHO. (2020) WHO information for the molecular detection of influenza viruses, January 06, 2021. *WHO webpage*, http://www.who.int/influenza/gisrs_laboratory/collaborating_centres/list/en/index.html.
(53) (2020) Instructions for the Laboratory Testing of COVID-19. *Chinese CDC*, http://www.chinacdc.cn/jkzt/crb/zl/szkb_11803/jszl_11815/202001/t20200123_20211379.html.

https://dx.doi.org/10.1021/acschembio.0c00840
ACS Chem. Biol. XXXX, XXX, XXX−XXX